

Evaluation of global land-to-ocean fresh water discharge and evapotranspiration using space-based observations

Ki-Weon Seo^{a,*}, Duane E. Waliser^b, Baijun Tian^{b,c}, James S. Famiglietti^d, Tajdarul H. Syed^{d,1}

^a Korea Polar Research Institute (KOPRI), KORDI, 406-840, Republic of Korea

^b Jet Propulsion Laboratory, California Institute of Technology, Pasadena, CA 91109-8099, USA

^c Joint Institute for Regional Earth System Science and Engineering, University of California, Los Angeles, CA 90095-7228, USA

^d Earth System Science, University of California, Irvine, CA 92697-3100, USA

ARTICLE INFO

Article history:

Received 9 May 2008

Received in revised form 2 February 2009

Accepted 14 May 2009

This manuscript was handled by K. Georgakakos, Editor-in-Chief, with the assistance of V. Lakshmi, Associate Editor

Keywords:

River discharge
Evapotranspiration
Remote sensing
GRACE

SUMMARY

We estimate global fresh water discharge from land-to-oceans (Q) and evapotranspiration (ET) on monthly time scales using a number of complimentary hydrologic data sets. This estimate is possible due to the new capability of measuring oceanic and land water mass changes from GRACE as well as the space-based measurements of oceanic and land precipitation (P_l) and oceanic evaporation. Monthly time series of Q show peaks in July and January, and those of ET show peaks in March, May and August. Our estimates of Q and ET are correlated with P_l indicating qualitatively that our estimates capture temporal patterns of Q and ET reasonably well. Comparison of our Q with two other previous estimates based on the Global Runoff Data Centre (GRDC) river gauges network shows that our maximum peak in Q occurs about a month later than previous estimates. In addition, we compare our estimation of Q and ET to 20th century simulations from the WCRP CMIP3 multi-model archive assessed in the IPCC 4th Assessment Report. Runoff (R) and ET from AOGCMs tend to only exhibit the annual cycle, but the Q estimated in this study exhibits additional semi-annual variations that exists in P_l as well. In addition, R from the models shows a maximum peak 2 months earlier than the estimated Q , which is due partly to the river discharge time lag that most AOGCMs do not take into account. These results indicate that current AOGCMs exhibit basic shortcomings in simulating Q and ET accurately. The new method developed here can be a useful constraint on these models and can be useful to close budget of global water balance.

© 2009 Elsevier B.V. All rights reserved.

Introduction

Evaluation of terrestrial water balance components, such as water storage changes ($\frac{dS_t}{dt}$), precipitation (P_l), evapotranspiration (ET) and fresh water discharge to oceans (Q), has been an important issue in terms of the global water and energy cycles, sediment transport and renewable water resources (e.g., Trenberth et al., 2007). Hence there have been many studies to estimate the terrestrial water balance components (e.g., Schlosser and Houser, 2007). Precipitation has been measured through in situ gauge observations and a combination of different remote sensing techniques (Adler et al., 2003; Xie and Arkin, 1997; Jaeger, 1983). Monthly terrestrial water storage changes have been measured with the Gravity Recovery and Climate Experiment (GRACE) launched March 2002 (Tapley et al., 2004).

However, limitations of direct measurements for Q and ET hinder their accurate global monitoring. The limitations for Q are, (1) the numbers of river gauges are declining globally, (2) surface water flows outside river channels where the gauges are installed (Alsdorf and Lettenmaier, 2003), (3) some river gauges are not located at the farthest downstream point and (4) river gauges cannot measure groundwater discharge (Dai and Trenberth, 2002). Accuracy in measuring ET is even worse than Q due to the lack of adequate micrometeorological networks and the difficulties in developing remote sensing approaches (Rodell et al., 2004).

Since water storage variations have become available from GRACE, there have been a few novel approaches to estimate monthly Q and ET for basin scales. Syed et al. (2007) calculated Q over the Mississippi and Amazon basins using the combined terrestrial and atmospheric water balance equation, and they extended their approach to the estimate of the globe (Syed et al., 2009). They were able to estimate Q from atmospheric precipitable water changes and the divergence of atmospheric moisture flux based on reanalysis as well as measurements of $\frac{dS_t}{dt}$. Rodell et al. (2004) estimated ET over the Mississippi basin from the measurements of $\frac{dS_t}{dt}$, P_l and Q . The methods of Syed et al. (2007) and Rodell

* Corresponding author. Address: Korea Polar Research Institute (KOPRI), 504 Get-Pearl Tower, 7-50 Songdo-Dong, Yeonsu-Gu, Incheon 406-840, Republic of Korea. Tel.: +82 32 260 6389.

E-mail address: seo.kiweon@kopri.re.kr (K.-W. Seo).

¹ Present address: Applied Geology, Indian School of Mines University, Dhanbad, India

et al. (2004) could be potentially extended to monitor global estimates of Q and ET based on the accumulation of evapotranspiration and fresh water discharge in river basins over the globe. However, the ET estimate by Rodell et al. (2004) includes the in situ measurement limitations of Q , and Syed et al. (2007) discussed that the error in atmospheric moisture flux from reanalysis impacted the accurate estimate of Q .

In this study, we evaluate *global* Q and ET on monthly time scales using a new approach without the influences from uncertainties in the estimations of atmospheric moisture flux from reanalysis or the in situ measurement limitations in Q . We also discuss anticipated error sources in our estimates.

Method

Fig. 1 shows a simplified diagram to represent the water cycle between land and oceans. Variations of terrestrial and oceanic water storage are balanced by precipitation, evaporation (evapotranspiration for land), and land-to-oceans freshwater discharge. It is important to note that Q is linked to both land and oceans as a sink and a source, respectively. Thus, on monthly time scales, Q can be estimated through the water balance equation over oceans.

$$Q = E_o - P_o + \frac{dS_o}{dt} \tag{1}$$

where $\frac{dS_o}{dt}$, P_o and E_o are monthly water storage changes, precipitation and evaporation over oceans, respectively. After Q is estimated, ET can be calculated through the water balance equation over land.

$$ET = P_l - Q - \frac{dS_l}{dt} \tag{2}$$

in which, P_l and $\frac{dS_l}{dt}$ are precipitation and water storage changes over land.

The benefit of this approach is using actual estimations of the water balance terms over oceans ($\frac{dS_o}{dt}$, P_o , and E_o) and land ($\frac{dS_l}{dt}$ and P_l), which are mostly based on observations by space-borne satellites. In particular, evaluations of Q and ET for monthly time scales are possible because GRACE started observing water storage variations over land and oceans since April 2002. Hence, the uncertainty from the estimation of the vapor flux divergence (Syed et al., 2007) or measurement of runoff at river gauges (Rodell et al., 2004) is avoided in such global estimates.

Data

Water storage changes

Water storage changes over oceans and land ($\frac{dS_o}{dt}$ and $\frac{dS_l}{dt}$) are estimated by GRACE gravity field retrievals. Since April 2002, GRACE has provided monthly gravity fields in the form of spherical harmonics and its life time is expected up to 2010 at least. The time-varying components in gravity are largely driven by water mass redistribution (Tapley et al., 2004). The current spatial reso-

lution of the time-varying GRACE products is about 1000 km, and the improved resolution is expected after the next reprocessing of GRACE data. Sub-monthly GRACE products are available with a compromise on poorer spatial resolution than the monthly products. In this study, we use the latest monthly GRACE product, CSR RL04 (Bettadpur, 2007). In time-varying GRACE products, there are two missing components of the gravity spectra due to GRACE measurement limitations and GRACE data processing, which are associated with the change of Earth center of mass and the average mass change (Bettadpur, 2007). First, because GRACE estimates gravity fields mainly based on the range-rate perturbations between twin satellites separated by about 200 km, it cannot provide gravity information caused by changes of the Earth center of mass. The redistribution of water mass between land and oceans is one of major forcings that perturb the Earth center of mass. As a result, this missing gravity spectrum is important to global-scale studies (Chambers et al., 2004), and thus we add this missing gravity spectrum component to GRACE data using Satellite Laser Ranging (SLR) measurements, which is sensitive to the variations of the Earth center of mass (Chen et al., 1999). Second, because the Earth is virtually a closed system, the mean gravity over the Earth does not vary with time. However, GRACE data processing removes the gravity effect associated with atmospheric surface pressure fields from GRACE products, and thus the time-varying GRACE products nominally represent water mass redistribution only between land and oceans. Consequently, mean gravity changes would be expected due to water flux from and to the atmosphere. We use precipitable water from the National Center for Environmental Prediction/National Center for Atmospheric Research (NCEP/NCAR) reanalysis (Kalnay et al., 1996) and calculate the average value for the entire Earth to compensate the missing mean gravity changes in the GRACE products. We also replace C_{20} gravity coefficient from GRACE with that estimated from the SLR because the error in the coefficient from GRACE is significant (Cheng and Tapley, 2004) likely due to aliasing from the mis-modeled S_2 atmospheric tide (Seo et al., 2008).

To estimate water storage variations from GRACE, we apply the dynamic filter of Seo et al. (2006) to suppress measurement noise. Fig. 2a shows a map of water storage anomalies in September 2005 with respect to a mean from 2003 to 2005. There are strong dipole signals in the tropical regions over land. From GRACE's measurements of water storage anomalies, we integrate water storage anomalies over all land and ocean areas and calculate their variations. Fig. 3a shows $\frac{dS_l}{dt}$ and $\frac{dS_o}{dt}$ observed by GRACE from September 2002 to November 2006. Clear seasonal cycles are present, and the phases between land and oceans are opposite. We also estimate measurement noise over land and oceans using GRACE's error variance provided with GRACE's gravity. Actual GRACE error is not known and the error level is likely larger than the estimated error (Wahr et al., 2006). However, the root mean square (RMS) noise over land and oceans during 51 months (September 2002–November 2006) are 4.394×10^{13} kg and 4.398×10^{13} kg, respectively, which are about two orders of magnitude smaller than signals from the same regions. This is because random noise is effectively reduced due to the averaging effect over the entire land and ocean areas. Besides gravity signals from water mass redistributions, GRACE can observe gravity changes associated with dynamics of solid earth such as earthquakes (Han et al., 2006) and post-glacial rebound (Barletta et al., 2008). However strong annual cycles of $\frac{dS_l}{dt}$ and $\frac{dS_o}{dt}$ in Fig. 3a exhibits that the signal of water mass redistribution between land and oceans is predominant and the effects from solid earth are very small during the examination period (2002–2007). Because GRACE is unique in its ability to measure water storage changes over land and oceans and its anticipated uncertainty is small compared both to the water storage signal and other uncertainties in precipitation and evaporation discussed following

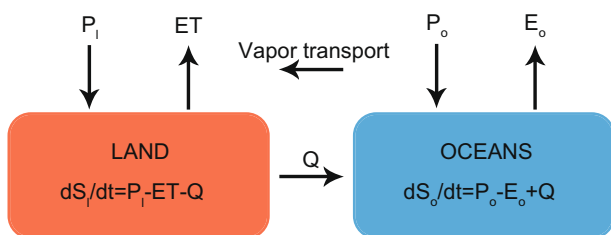


Fig. 1. A schematic diagram of water cycles between land and oceans.

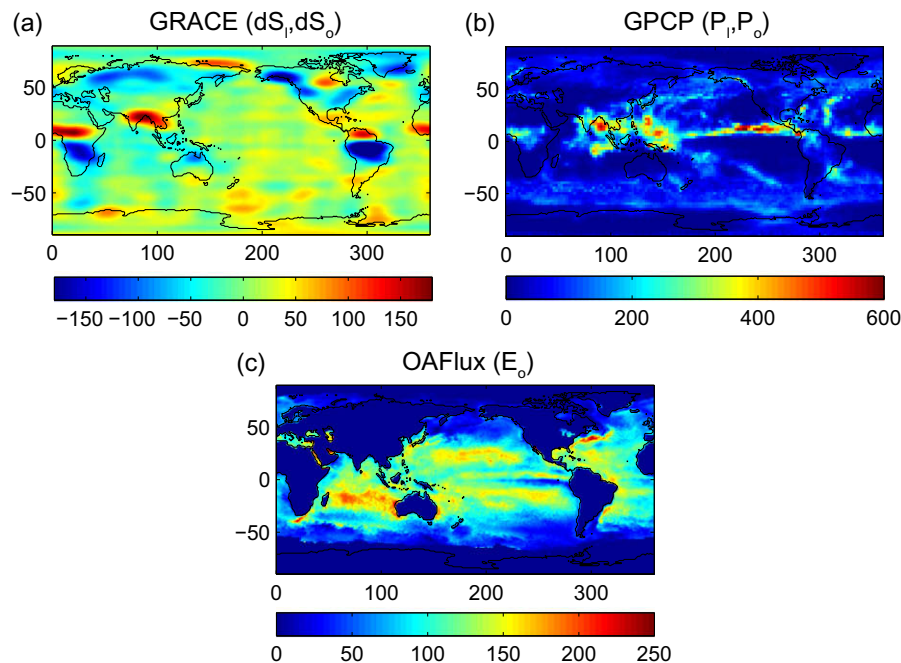


Fig. 2. Global fields of (a) water storage variations, (b) precipitation (c) and evaporation in September 2005. Units are mm of water.

sections, we assume the error in $\frac{dS_l}{dt}$ and $\frac{dS_o}{dt}$ to be negligible in *global* Q and ET estimates.

Although amplitudes of $\frac{dS_l}{dt}$ and $\frac{dS_o}{dt}$ are small compared to those of precipitation and evaporation (discussed in the next sections), their monthly variations play an important roles in estimating month-to-month variations of *global* Q and ET . This is because the amplitude of difference between precipitation and evaporation is comparable to that of water storages. Therefore, without GRACE measurements of the water storage, incorrect monthly variations of *global* Q and ET may be calculated.

Precipitation

For precipitation over oceans and land (P_o and P_l), we use the Global Precipitation Climatology Project (GPCP) data (Adler et al., 2003) and the CPC Merged Analysis of Precipitation (CMAP) (Xie and Arkin, 1997). GPCP data is a merged product to take advantage of each different type of precipitation data, which are (1) microwave estimates based on Special Sensor Microwave/Imager (SSM/I), (2) infrared estimates from geostationary and polar orbiting satellites, (3) the estimates from the Outgoing Longwave Radiation Precipitation Index (OPI) data, and (4) the in situ gauge data. Monthly GPCP products are available from February 1979 to the present with $2.5^\circ \times 2.5^\circ$ spatial resolution. Similar to GPCP, CMAP is a merged estimate with rain gauges and retrievals of satellite-borne microwave and infrared sensors. CMAP is also available from 1979 to the present with $2.5^\circ \times 2.5^\circ$ spatial resolution.

Fig. 2b shows monthly GPCP precipitation rate for September 2005. Dominant precipitation is observed over oceans near equator in northern hemisphere. Red lines in Fig. 3b and c show P_l and P_o from GPCP, respectively, for GRACE period. Blue lines in the same plots are P_l and P_o from CMAP. In general, $P_o(P_l)$ in GPCP is smaller (greater) than $P_o(P_l)$ in CMAP while their month-to-month variations agree very well. Correlation coefficients between GPCP and CMAP for land and oceans are 0.97 and 0.85, respectively. Biases in precipitation products observed in the monthly time series of GPCP and CMAP could hinder accurate estimate of Q and ET . This is because biases are not canceled out in contrast to random noise during integration of precipitation over the entire land and ocean

areas. Therefore, we estimate Q and ET using both GPCP and CMAP and examine how values of Q and ET differ due to the uncertainty in precipitation data sets.

Evaporation

To estimate evaporation over oceans (E_o), we use the Objectively Analyzed Air-Sea Fluxes (OAFlex) (Yu et al., 2004) and Hamburg Ocean Atmosphere Parameters and fluxes from Satellite data (HOAPS) (Shulz et al., 1997). They are developed by integrating space-based observation with in situ measurements and reanalysis. For example, evaporation in the OAFlex product is estimated using a bulk formula based on wind speed, air humidity, air temperature, and sea surface temperature. These meteorological variables are derived from a combination of satellite retrievals and weather analysis, such as European Center for Medium-range Weather Forecasts (ECMWF) and NCEP/NCAR reanalyses. There exist other oceanic evaporation products based on satellite remote sensing, for example GSSTF2 (Chou et al., 2003). However, periods of other products do not overlap with GRACE, and thus we do not use them here.

Fig. 2c shows monthly OAFlex evaporation rate over oceans for September 2005. There is strong evaporation in the Southern Indian Ocean. It is important to note that evaporation is not available in high-latitude oceans because of spatial coverage of satellite remote sensing capabilities obscured by sea-ice. Sea-ice extent varies seasonally and thus the missing-data areas changes accordingly. For example, OAFlex does not include above around 60°S in September and around 70°S in February. One expects that the amplitude of, and thus the contribution from, the missing evaporation is very small compared to that of global oceans. However, as stated in the previous section, budgets of Q and ET are small compared particularly to that of E_o , thus the incomplete global coverage of evaporation probably impacts on our estimate. To consider this, we use evaporation from NCEP/NCAR reanalysis over the high latitude oceans where OAFlex and HOAPS do not include. We estimate Q and ET with and without the high-latitude NCEP/NCAR evaporation. Fig. 3d shows E_o from OAFlex (red line) and HOAPS (blue line). The two products agree well during their overlap (the

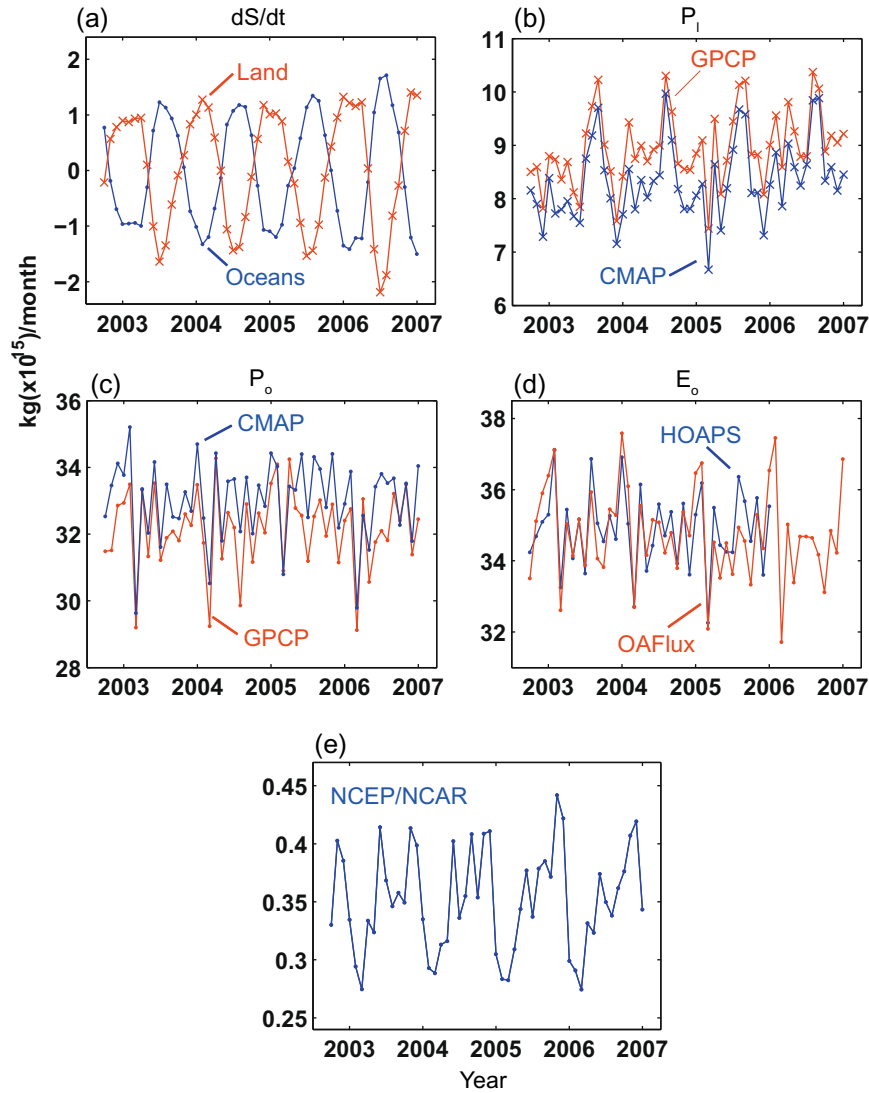


Fig. 3. (a) shows water mass changes over oceans and land from GRACE; (b, c) represent precipitation over land and oceans, respectively; (d) shows evaporation over oceans; (e) shows evaporation in the high latitude oceans where OAFflux and HOAPS do not include.

correlation coefficient is 0.80); HOAPS product is available only up to 2005. We use the two monthly time series of E_o to evaluate Q and ET . Fig. 3e shows the evaporation of NCEP/NCAR from the high latitude oceans to illustrate that it is about two orders of magnitude smaller than those in Fig. 3d, and thus its impact on the global value is very little.

Results and discussion

Annual amplitude of global Q and ET

Combinations of available hydrological data provide eight different estimates of Q and ET . Tables 1 and 2 summarize annual means of them from 2003 to 2005. Table 1 represents annual

amplitudes of Q and ET in the case of adding NCEP/NCAR evaporation for the missing high latitude oceans. Annual means of Q and ET vary from 2.50×10^{16} kg/yr to 3.63×10^{16} kg/yr and 7.01×10^{16} kg/yr to 7.39×10^{16} kg/yr, respectively. Schlosser and Houser (2007) showed many Q estimates from the literatures from 1905 to the present. Its variations range around from 2.50×10^{16} kg/yr to 4.75×10^{16} kg/yr, and our estimates are within the range. Table 2 represents annual amplitudes of Q and ET without the NCEP/NCAR evaporation. Amplitudes of Q (ET) are smaller (larger) than those in Table 1. Amplitudes of NCEP/NCAR evaporation in the high latitude oceans account for about 1% compared to those of OAFflux and HOAPS in the rest of oceans (shown in Fig. 3d and e), but they affect Q and ET estimates significantly about 16% and 6%, respectively. The relatively large scatter is caused by different precipitation

Table 1

Annual amplitudes (kg/yr ($\times 10^{16}$)) of Q and ET based on different data. Evaporation at high latitude oceans where OAFflux and HOAPS do not include is calculated from NCEP/NCAR evaporation.

	GRACE/GPCP/OAFflux	GRACE/CMAP/OAFflux	GRACE/GPCP/HOAPS	GRACE/CMAP/HOAPS
Q	3.49	2.50	3.63	2.64
ET	7.16	7.39	7.01	7.24

Table 2
Annual amplitudes ($\text{kg/yr} (\times 10^{16})$) of Q and ET based on different data. Evaporation at high latitude oceans where OAFflux and HOAPS do not include is not taken into account.

	GRACE/GPCP/OAFflux	GRACE/CMAP/OAFflux	GRACE/GPCP/HOAPS	GRACE/CMAP/HOAPS
Q	3.07	2.08	3.21	2.22
ET	7.58	7.81	7.43	7.67

and evaporation data. Considerable impact from the evaporation in the high latitude oceans, particularly on Q , implies that caution must be necessary to estimate magnitudes of Q and ET . In particular, this attention is likely true when comparing the historical Q estimates summarized by Schlosser and Houser (2007) with those evaluated here. Although our Q estimates are within the range of the previous studies, they lie around the lower values of previous estimates due probably to biases in precipitation and evaporation.

Monthly time series of global Q and ET

We examine month-to-month variations of Q and ET from September 2002 to November 2006. Fig. 4 shows the monthly time

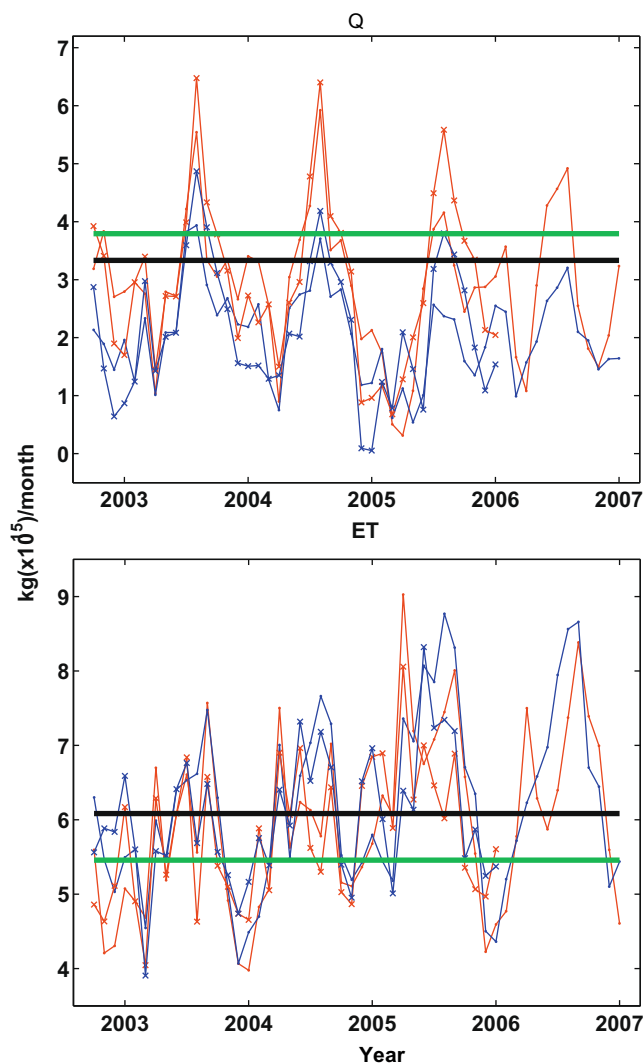


Fig. 4. Estimated Q and ET in monthly time scales. The red-dot, blue-dot, red-cross and blue-cross represent estimates using GPCP + OAFflux, CMAP + OAFflux, GPCP + HOAPS and CMAP + HOAPS, respectively. GRACE data is commonly used in the four plots. The black and green lines are estimates from Trenberth et al. (2007) and Oki and Kanae (2006), respectively. (For interpretation of the references to color in this figure legend, the reader is referred to the web version of this article).

series of Q and ET . The red-dot, blue-dot, red-cross and blue-cross represent estimates from GRACE + GPCP + OAFflux, GRACE + CMAP + OAFflux, GRACE + GPCP + HOAPS and GRACE + CMAP + HOAPS, respectively. Those plots include effect of NCEP/NCAR evaporation in the high latitude oceans. Without the NCEP/NCAR evaporation, time series (not shown) are very similar to Fig. 4 since peak-to-peak variations of evaporation in the high-latitude oceans is only approximately $0.15 \times 10^{15} \text{ kg}$ (Fig. 3e). Trenberth et al. (2007) and Oki and Kanae (2006) estimated long-term annual mean Q and ET , showing $4.00 \times 10^{16} \text{ kg/yr}$ and $4.55 \times 10^{16} \text{ kg/yr}$ for Q and $7.30 \times 10^{16} \text{ kg/yr}$ and $6.55 \times 10^{16} \text{ kg/yr}$ for ET , respectively. Here we simply divide their estimates by 12 for monthly means, and plot in the blue and black lines in the figure. Our mean estimates from Table 1 for Q and ET are $3.07 \times 10^{16} \text{ kg/yr}$ and $7.20 \times 10^{16} \text{ kg/yr}$, respectively. In general, while our ET estimates are similar to the estimate by Trenberth et al. (2007), our Q estimates are smaller than the previous studies. This is probably due to different observational time periods and different data in this and previous studies. For example, Syed et al. (2009) used GRACE and reanalyses from 2003 to 2005 to estimate the annual mean of Q . Their estimate ($3.23 \times 10^{16} \text{ kg/yr}$) is very close to our Q . This is likely due to the common time span between the two studies. On the other hand, Trenberth et al. (2007) used reanalyses data from 1979 to 1995 and gauge data whose measurement time spans are highly variable to estimate Q . Thus, inter-annual and decadal variations in Q could possibly contribute to some of the differences. In addition, uncertainties in remote-sensed E_o , P_o and P_i will propagate to our Q and ET estimations. Similarly, previous studies may be affected by limitations of in situ measurement.

Monthly time series of Q show strong annual cycles with a maximum in July. Those of ET do not show a sharp peak at a particular month, but there are annual cycles with maxima during boreal summer. For Q , and for this relatively short period, there appears to be little evidence of a robust trend – apart from indications of a small negative trend during boreal summers and the significant drop in early 2005. The time series of ET indicates a positive trend. This increase in ET is likely in part related to the positive trend in the observed P_i (Fig. 3b).

Annual cycles of global Q and ET

To illustrate the annual variations more clearly, the mean annual cycle for Q and ET are calculated from the time series in Fig. 4 and are illustrated in the top panels of Fig. 5. In addition, the annual cycles of E_o , P_o and P_i , which are used to estimate the Q and ET , are shown in the bottom panel of Fig. 5. For Q and ET , we use the same symbols in Fig. 4 and add thick black lines to indicate means of the four estimates. In the bottom panel, the annual cycles are from means of two corresponding products for P_o and P_i (GPCP + CMAP) and for E_o (OAFflux + HOAPS). For the plots of annual cycles of E_o , P_o and P_i , their means are removed to better compare their amplitudes and phases in a single panel. The annual cycle of Q more clearly exhibits a major peak in July and a minor peak in January. These peaks are correlated with peaks in the annual cycle of P_i ; their correlation coefficient is 0.76. Our Q is estimated without P_i but exhibits a good correlation with P_i , indicating our result captures temporal variations of Q reasonably. From these Q estimates, there is about a factor of four changes in Q

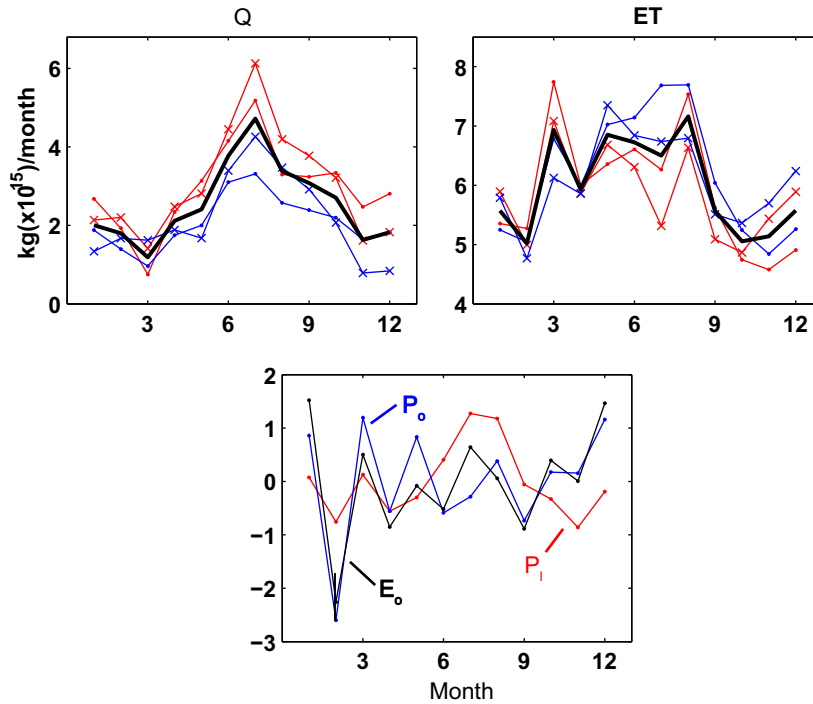


Fig. 5. Annual cycles of Q and ET derived from this study and P_i , P_o and E_o which are used to estimate the Q and ET . The Q and ET have good correlations with P_i .

over the course of the annual cycle, reaching a maximum of ~ 4.7 in July and a minimum of ~ 1.2 in March. It is not certain that this July peak is driven by the July peak in P_i because the phases of Q and P_i need not necessarily be the same. Peaks of river discharge from drainages located at high latitude may happen earlier than those of precipitation due to snow melt in spring (Dai and Trenberth, 2002). On the other hand, there is a time lag between the two peaks resulting from the travel time of runoff to the oceans in large drainages. The annual cycle of ET shows significant peaks in March, May and August and in general has a good agreement with that of P_i (the correlation coefficient is 0.69), which is the similar case of the correlation between E_o and P_o (the correlation coefficient is 0.87). We compare our annual cycle of Q to two previous studies in Fig. 6. Our estimate is the black line, and results from Dai and Trenberth (2002) and Fekete et al. (2002) are the blue and the red lines, respectively. The two previous estimates are based on GRDC river gauge measurements, which are not exactly discharge or runoff because their gauges are not installed at the farthest

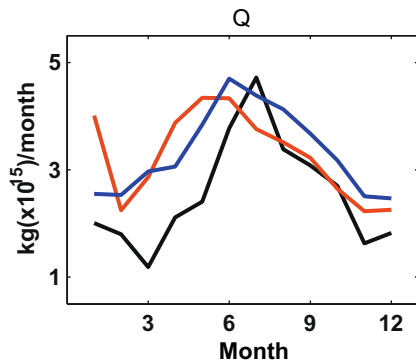


Fig. 6. Annual cycles of three different estimates of Q . Black line denotes our Q , and blue and red lines represent Q from Dai and Trenberth (2002) and Fekete et al. (2002), respectively. (For interpretation of the references to color in this figure legend, the reader is referred to the web version of this article).

downstream of river channels. Dai and Trenberth (2002) used a river transport model for the discharge estimation. As a result, both the black line (our estimate) and the blue line (Dai and Trenberth (2002)'s estimate) represent land-to-oceans fresh water discharge. On the other hand, Fekete et al. (2002) used a water balance model to calculate composite runoff field at global grids. Therefore, a non-zero phase difference, accounting for travel time of runoff field to reach the oceans, is expected between the red line and the others. This expectation is born out by the earlier maximum peak of the red line compared to the others. In addition, the blue line shows a peak in June while the black line does two peaks in July and January. July and January roughly represent summer wet seasons for Northern Hemisphere and Southern Hemisphere, respectively. Similarly, two peaks are also observed in the red line, but the January peak is significantly larger than our estimate. The 1 month phase lag in the black line compared to the blue line is due probably to the contribution of submarine discharge, which is groundwater discharge to oceans. River gauges cannot measure the submarine discharge, but our estimate includes it in water balance equations. Other than the phase difference between this study and previous studies, the shape of annual cycle for Q in this study is sharper than others while it is expected that spectrum of Q here (considering surface and subsurface runoff) should be more significant at lower frequency than others (only considering surface runoff). Because our estimate is based on time span only from 2002 to 2007, and previous studies used river gauge data mostly before 2000 and for more than a couple of decades, inter-annual and decadal variation of Q may explain the differences between this study and others. As the result, this discussion is preliminary and further examination is necessary.

Given these estimates represent a new approach to evaluate global Q and ET , it is worthwhile to use them to assess the representation of global Q and ET in contemporary global atmosphere-ocean-land coupled climate models (AOGCMs). In this case we compare our estimation of global Q and ET to global runoff (R) and ET from model output based on the WCRP CMIP3 multi-model archive at PCMDI from simulations of 20th century conditions

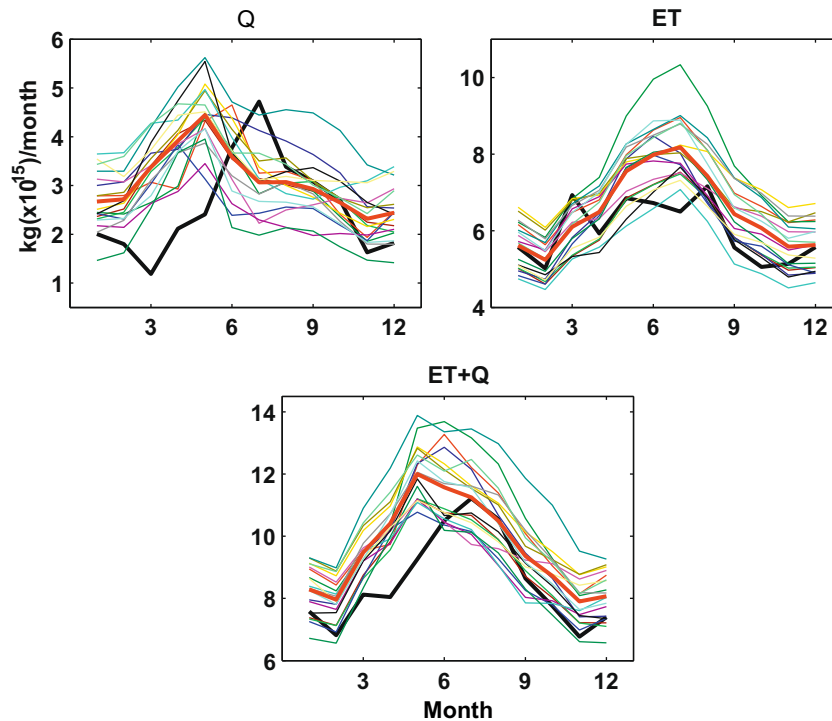


Fig. 7. Annual cycles of Q , ET and $Q + ET$ from this study (thick black lines), R , ET , and $R + ET$ from AOGCMs model output (thin colored lines) and ensemble means of model outputs (thick red lines). R and ET from models show only dominant seasonal cycles, and Q and ET from this study show both seasonal and sub-seasonal cycles. (For interpretation of the references to color in this figure legend, the reader is referred to the web version of this article.)

(Meehl et al., 2007) that was utilized in the 4th Assessment Report by the IPCC (2007). Because most AOGCMs do not incorporate river routing models, we use the *global runoff* as a quantity of Q . As the result, there is no time lag associated with river flow to the oceans for the R from AOGCMs, while Q estimated via the remote sensing observations is the discharge from land-to-oceans. Consequently, there is expected to be a phase difference between our Q and model's R even though both the observation and the simulation might be a realistic representation. Fig. 7 presents annual cycles of *global* Q , ET and $Q + ET$ from this study (thick black lines), *global* R , ET and $R + ET$ from each of the model simulations (thin colored lines) and the multi-model ensemble mean (thick red lines). The annual cycle of R from the AOGCMs only exhibits annual variations, having a peak at the month of May – 2 months prior to the peak in the observed Q . The phase difference is partly due to the river discharge time lag.

For ET , in general our estimate and AOGCMs' output show the similar annual component. Both show strong ET from boreal spring to fall. As with Q , the annual cycle of the satellite-based estimate of ET exhibits both annual and semi-annual components, while the modeled values tend to only exhibit the annual variation. The bottom panel of Fig. 7 shows the sums of Q (R for models) and ET . Both the models and the observation display similar temporal variation but still with a 2-month phase difference during the peak value. The similar temporal variations of $Q + ET$ ($R + ET$ for models) indicate that the error in Q (or R) and ET occurs in separating terrestrial water from P_i into Q (or R) and ET . This is more likely to be the case for the models because (1) accurate simulations of ET and snowmelt are challenging in the models (Shuttleworth, 2007; Niu et al., 2005) and (2) our estimate of Q and ET are in good agreement with P_i . However, it is not possible yet to assess rigorously the relative accuracies for the Q (R for models) and ET between our estimate and AOGCMs because, apart from the error in the models, our Q and ET estimates are possibly contaminated by errors in remote sensing data. Nevertheless, similar temporal variations between

our Q and P_i and between our ET and P_i suggest that the estimates based on satellite remote sensing are possibly more realistic representations of *global* Q and ET than those from the models. Therefore, *global* Q and ET evaluated in this study are potentially a useful constraint for developing and validating contemporary global climate models.

Conclusions

We estimate *global* Q and ET in monthly time scales from September 2002 to November 2006 using satellite-borne remote sensing and water balance equations between land and oceans. For the satellite observations, we adopt GRACE's time varying gravity to calculate water storage variations, two global precipitation products (GPCP/CMAP) and two global oceanic evaporation products (OAFflux/HOAPS). Because OAFflux and HOAPS do not include high latitude oceans, we use NCEP/NCAR evaporation to account for the missing region. Using all combinations of the different data sets, we are able to make eight observational-based estimates of *global* Q and ET . Their values, with their differences providing a measure of uncertainty, are within the range of previous estimates based on more traditional techniques. The relatively large variations of annual amplitudes of the Q and ET indicate that they are vulnerable to small biases in other hydrological components. We compare annual cycles of Q and ET to previous estimates and AOGCM's output. Our estimates show both annual and semi-annual components while others only show annual components. The good agreements of our Q and ET with P_i indicate that the new estimates are reasonable and possibly useful to validate current AOGCMs.

Acknowledgements

This study was supported by the NASA Postdoctoral Program (NPP), Korea Polar Research Institute (KOPRI) projects (PE09020,

PG08010), the NASA Earth System Science Fellowship Program, and the NASA NEWS and Modeling, Analysis and Prediction Programs. In addition, the second and third authors' contributions to this study were carried out on behalf of the Jet Propulsion Laboratory, California Institute of Technology, under a contract with the National Aeronautics and Space Administration (NASA).

References

- Adler, R.F., Huffman, G.J., Chang, A., Ferraro, R., Xie, P.-P., Janowiak, J.E., Rudolf, B., Schneider, U., Curtis, S., Bolvin, D., Gruber, A., Susskind, J., Arkin, P.A., Nelkin, E., 2003. The version 2 Global Precipitation Climatology Project (GPCP) monthly precipitation analysis (1979–present). *J. Hydrometeorol.* 4, 1147–1167.
- Alsdorf, D.E., Lettenmaier, D., 2003. Tracking fresh water from space. *Science* 301, 1491–1494.
- Barletta, V., Sabadini, R., Bordon, A., 2008. Isolating the PGR signal in the GRACE data: impact on mass balance estimates in Antarctica and Greenland. *Geophys. J. Int.* 172 (1), 18–30.
- Bettadpur, S., 2007. GRACE UCSR Level-2 Processing Standards Document for Level-2 product release 0004, 17 pp.
- Chambers, D.P., Wahr, J., Nerem, R.S., 2004. Preliminary observations of global ocean mass variations with GRACE. *Geophys. Res. Lett.* 31, L13310. doi:10.1029/2004GL020461.
- Chen, J.L., Wilson, C.R., Eanes, R.J., Nerem, R.S., 1999. Geophysical interpretation of observed geocenter variations. *J. Geophys. Res.* 104 (B2), 2683–2690.
- Cheng, M., Tapley, B.D., 2004. Variations in the Earth's oblateness during the past 28 years. *J. Geophys. Res.* 109, B09402. doi:10.1029/2004JB003028.
- Chou, S.-H., Shie, C.-L., Atlas, B., Ardizzone, J., 2003. Surface turbulent heat and momentum fluxes over global oceans based on Goddard satellite retrievals, Version 2 (GSSTF2). *J. Clim.* 16, 3256–3273.
- Dai, A., Trenberth, K.E., 2002. Estimates of freshwater discharge from continents: latitudinal and seasonal variations. *J. Hydrometeorol.* 3, 660–687.
- Fekete, B.M., Vorosmarty, C.J., Grabs, W., 2002. High resolution fields of global runoff combining observed river discharge and simulated water balances. *Global Biochem. Cycles* 16 (3). doi:10.1029/1999GB001254.
- Han, S.-C., Shum, C., Bevis, M., Ji, C., 2006. Crustal dilatation observed by GRACE after the 2004 Sumatra-Andaman earthquake. *Science* 313, 658–662.
- IPCC, Climate change 2007. The Physical Science Basis, IPCC Secretariat, Geneva, Switzerland.
- Jaeger, L., 1983. Monthly and areal patterns of mean global precipitation. In: Street-Perrott, A., Beran, M., Ratcliffe, R. (Eds.), *Variations in the Global Water Budget*. D. Reidel Publ. Co., Dordrecht., pp. 129–140.
- Kalnay, E. et al., 1996. The NCEP/NCAR 40-year reanalysis project. *Bull. Am. Meteorol. Soc.* 77 (3), 437–471.
- Meehl, G.A., Covey, C., Delworth, T., Latif, M., McAvaney, B., Mitchell, J.F.B., Stouffer, R.J., Taylor, K.E., 2007. The WCRP CMIP3 multi-model dataset: a new era in climate change research. *Bull. Am. Meteorol. Soc.* 88 (9), 1383–1394.
- Niu, G.-Y., Yang, Z.-L., Dickinson, R.E., Gulden, L.E., 2005. A simple TOPMODEL-based runoff parameterization (SIMTOP) for use in global climate models. *Geophys. Res. Lett.* 110, D21106. doi:10.1029/2005JD006111.
- Oki, T., Kanae, S., 2006. Global hydrological cycles and world water resources. *Science* 313, 1068–1072.
- Rodell, M., Famiglietti, J.S., Chen, J., Seneviratne, S.I., Viterbo, P., Holl, S., 2004. Basin scale estimates of evapotranspiration using GRACE and other observations. *Geophys. Res. Lett.* 31, L20504. doi:10.1029/2004GL020873.
- Schlosser, C.A., Houser, P.R., 2007. Assessing a satellite-era perspective of the global water cycle. *J. Clim.* 20 (7), 1233–1246.
- Seo, K., Wilson, C.R., Famiglietti, J.S., Chen, J., Rodell, M., 2006. Terrestrial water mass load changes from Gravity Recovery and Climate Experiment (GRACE). *Water Resour. Res.* 42, W05417. doi:10.1029/2005WR004255.
- Seo, K., Wilson, C.R., Chen, J., Waliser, D.E., 2008. GRACE's spatial alias error. *Geophys. J. Int.* 172 (1), 41–48.
- Shulz, J., Meywerk, J., Ewald, S., Schlüssel, P., 1997. Evaluation of satellite-derived latent heat fluxes. *J. Clim.* 10, 2783–2795.
- Shuttleworth, W.J., 2007. Putting the 'vap' into evaporation. *Hydrol. Earth Syst. Sci.* 11 (1), 210–244.
- Syed, T.H., Famiglietti, J.S., Zlotnicki, V., Rodell, M., 2007. Contemporary estimates of Pan-Arctic freshwater discharge from GRACE and reanalysis. *Geophys. Res. Lett.* 34, L19404. doi:10.1029/2007GL031254.
- Syed, T.H., Famiglietti, J.S., Chambers, D.P., 2009. GRACE-based estimates of terrestrial freshwater discharge from basin to continental scales. *J. Hydrometeorol.* 10 (1), 22–40. doi:10.1175/2008JHM993.1.
- Tapley, B.D., Bettadpur, S., Ries, J.C., Thompson, P.F., 2004. GRACE measurements of mass variability in the Earth system. *Science* 305, 503–505.
- Trenberth, K.E., Smith, L., Qian, T., Dai, A., Fasullo, J., 2007. Estimates of the global water budget and its annual cycle using observational and model data. *J. Hydrometeorol.* 8 (4), 758–769.
- Wahr, J., Swenson, S., Velicogna, I., 2006. Accuracy of GRACE mass estimates. *Geophys. Res. Lett.* 33, L06401. doi:10.1029/2005GL025305.
- Xie, P., Arkin, P.A., 1997. Global precipitation: A 17-year monthly analysis base on gauge observation, satellite estimates, and numerical model outputs. *Bull. Am. Meteorol. Soc.* 78, 2539–2558.
- Yu, K., Weller, R.A., Sun, B., 2004. Improving latent and sensible heat flux estimates from the Atlantic Ocean (1988–1999) by a synthesis approach. *J. Clim.* 17, 373–393.